3D imaging of transparent objects

A. M. Wallace, P. Csakany
Dept. of Computing and Electrical Engineering
G. S. Buller, and A. C. Walker
Dept. of Physics
Heriot Watt University
Edinburgh, Scotland

Abstract

In spite of the rapid growth in the application of active 3D sensing technologies, it has proved difficult to acquire surface data from transparent objects due to the high transmittance and specularity of the surfaces and the confusion caused by multiple returns. In this paper, we describe how active time-of-flight range sensing using photon counting can be used to acquire data from several transparent surfaces simultaneously.

Following a short introduction, the paper is organised in three main sections. First we review the basic principles of time of flight ranging using time correlated single photon counting. Second, we present some basic theory of how data is acquired from multiple surfaces. Third, we present some initial measurements on common transparent objects. Finally, we summarise progress and the necessity for further work.

1 Introduction

In the last decade, active laser 3D imaging systems have moved from the development stage [1] to widespread application in the manufacturing, design, multimedia and leisure industries [2, 3]. Triangulation systems are the clear market leader because they can provide rapid data acquisition to a well understood tolerance. However, they have several limitations. First, their accuracy is determined by the triangular geometry and sensor resolution. Second, the separation of projector and camera makes occlusion inevitable on any surface with significant concavities. These two factors often lead either to a completely different system for each scale of measurement, or to hybrid systems which use a combination of mechanical and triangulation sensing to measure 3D data points. Finally, triangulation systems are sensitive to the reflectance properties of the material; poorly or specularly reflecting materials can result in no or multiple returns. In practice, it is not uncommon to use a matt white coating to measure 'difficult' objects.

TOF systems are less widespread, due primarily to the difficulty in resolution of the short time intervals necessary to measure depth accurately in a medium (usually air) in which light travels $1mm$ in approximately $3.3ps$. Broadly, these systems can be divided into pulsed, amplitude modulated (AM) and frequency modulated (FM) systems. In a pulsed system, a range resolution of $\pm 2mm$ at ranges up to 30 metres is typical. The limiting factor is the rise time in the detected pulse. In an AM system, the phase change

BMVC 2000 doi:10.5244/C.14.47

between a continuously modulated laser reference and the target signal is measured, resulting in a typical accuracy of $\pm 1mm$ or slightly better over a similar range. In an FM system, a laser diode's optical frequency is modulated and again the range is proportional to the measured phase change between the reference and target signal during a round trip. Of these techniques, this appears to give the most accurate results, $\pm 0.1mm$ at best. In general, these systems do not measure well distance from surfaces of non-uniform reflectance, as they suffer from 'range-intensity' crosstalk, that is the comparison of the target against the necessary reference is affected adversely by variations in amplitude between the signals.

In previous work, we have developed a new approach to time-of-flight laser ranging, reviewed briefly in the next section, which improves on the accuracy and sensitivity of existing techniques [4]. In this paper we address the potential of our approach to solve a neglected problem, that of acquiring 3D data from and imaging transparent surfaces. In so doing, we also consider whether data can be acquired not only from the first surface encountered by the projected laser signal, but also from subsequent surfaces in its path. Of course, there are many practical instances of inspection of transparent objects, such as bottles, but these rely on workstations with complex lighting to effectively produce binary images and reduce the problem to 2D inspection; there is no attempt to image the surface. Full 3D surface measurement of transparent surfaces is the goal of the current work. [1]

2 3D imaging by time correlated single photon counting

Time-correlated single photon counting (TCSPC) is a well established technique [5] which has been applied previously to time-resolved fluorescence and fibre-based optical time domain reflectometry measurements. A schematic diagram and a photograph of a time of flight (TOF) ranging system using TCSPC are illustrated in figure 1. The laser source is a passively Q-switched AlGaAs-GaAs laser diode which emits 10 - $20ps$ pulses of energy $\approx 10pJ$ at 850 nm and a repetition frequency of up to $25MHz$. A fraction of each optical pulse is split off and sent to a trigger detector, an avalanche photodiode (APD), which provides a START signal. Photons scattered from either the target or reference are detected by an actively-quenched single photon avalanche diode (SPAD) which provides the STOP input. In the time-to-amplitude convertor (TAC) a linear ramp is started by the APD and stopped by the SPAD so that the photon arrival time is converted to a voltage. This is converted by the analogue-to-digital convertor (ADC) and recorded by the multi-channel analyser (MCA) previous to storage in computer memory.

The distance measurement is obtained from the separation of the target and reference signals from the SPAD. In these measurements, the reference channel is an optical fibre of known path length. Since only one photon is detected from each transmitted laser pulse, each detected photon event is an independent measure of distance. The timing accuracy, and hence depth resolution, can then be improved by repeating the measurement from 10 to 10^7 times. The separation of the peaks formed from the accumulated photon returns of the target and reference channels defines the distance to the target.

The system can provide occlusion-free, dense depth images directly from a surface with accuracies superior to current TOF systems which use pulsed, AM or FM modula-

[1] An internet search reveals several examples of automated inspection of glass objects, for example www.ipsautomation.com, www.filtec.com

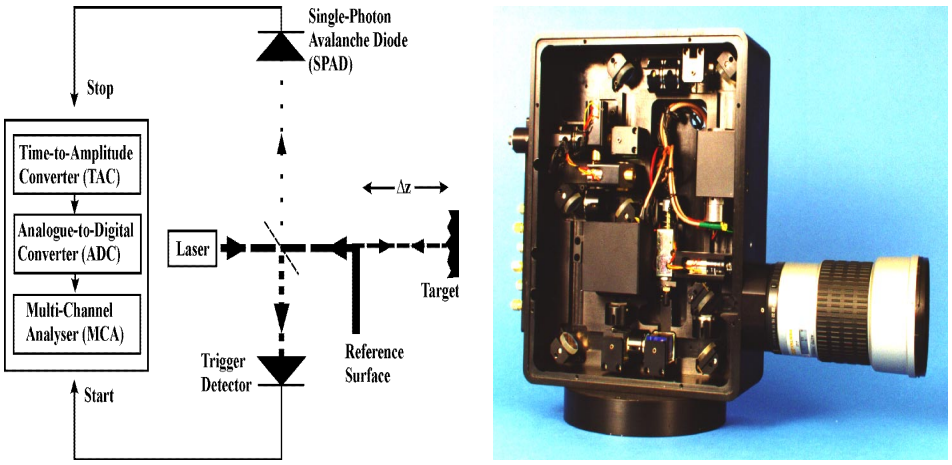

(a) Schematic diagram (b) Photograph

Figure 1: The TOF-TCSPC sensor

tion. In summary, the sensor has the following characteristics.

- Absolute measurement of range to an accuracy and repeatability of $15um$
- Measurement in 3 dimensions using existing scanning to better than $\pm 0.1mm$
- Measurement of objects from less than $5cm$ to about $25m$ in size
- Measurement directly from the object surface, rather than from targets or retro-reflectors
- Robust and portable to allow imaging of large components in situ
- Automatic surface scanning from many different surface materials
- Automatic channel equalization and auto-focussing
- Eye-safe class 1 laser operation

Two examples of the histograms formed from accumulated photon counts are illustrated in figure 3. The vertical axis defines the number of accumulated photon counts in each channel which is defined by the horizontal axis. The channel resolution is $2.44ps$ per channel throughout the paper. In figure 3(a) the peak on the left is from an opaque target surface and the peak on the right from the optical fibre. The number of counts in each channel c_i follows a Poisson probability distribution with mean n_i and variance n_i where n_i is the number of observed counts in channel c_i. There is a small dark count which can be estimated easily, and a correction for pulse pile-up is also applied [4]. Previously, we favoured the fit of an operating model, a product of two functions (a Lorentzian and a polynomial), to the sidelobe of the autocorrelation function formed from the raw histogram [6]. However, we obtained only slightly less accurate results by upsampling and fitting a simple second order polynomial. Figure 3(b) shows an example of a photon return from a transparent object depicted in figure 2(a), a floppy disk box. The reference peak is on the far right, the other three peaks are, from left to right, the returns from the front and rear surfaces of the box then from a sheet of cardboard placed behind it.

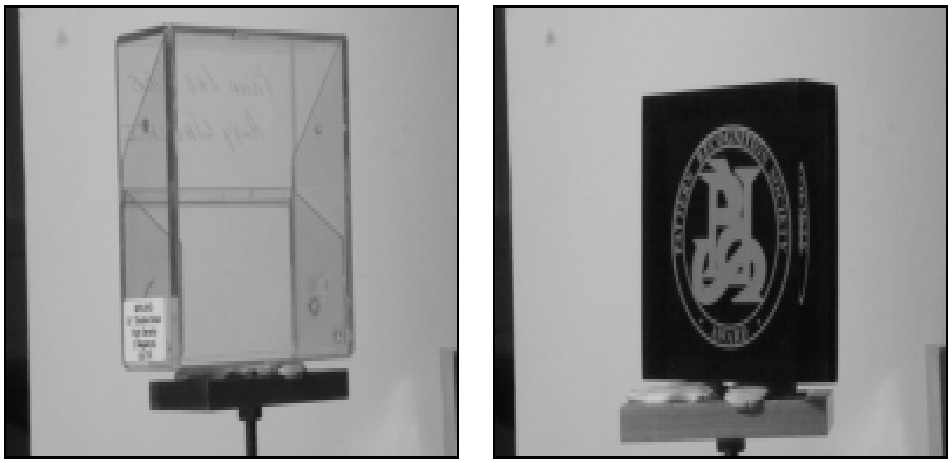

(a) Computer floppy disk box (b) Pattern Recognition paperweight

Figure 2: Examples of transparent objects

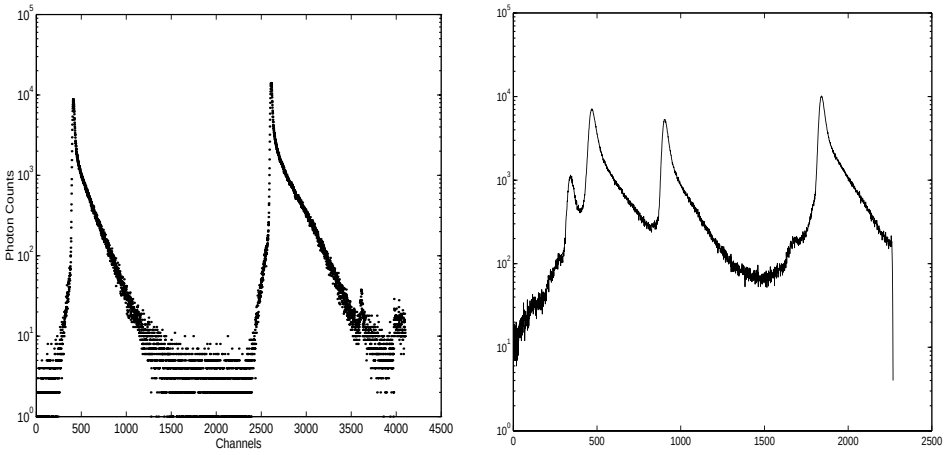

(a) Opaque (b) Transparent

Figure 3: Photon count histogram data from opaque and transparent objects

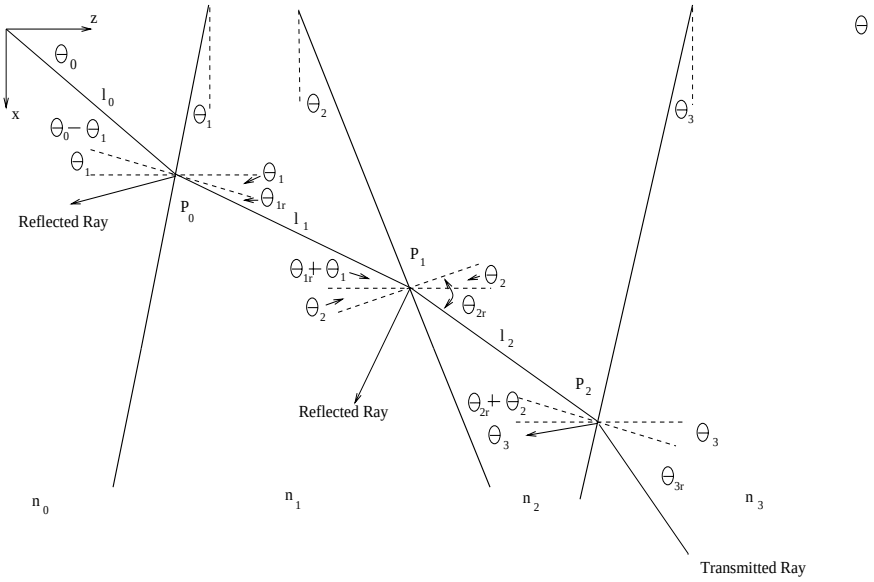

Figure 4: Transmission and reflection of light through several media

3 Transmission of light through several media

In general, there are two principal problems we wish to address. First, can we get enough signal return to make depth measurement from transparent surfaces a realistic proposition ? Second, can we determine the (x, y, z) coordinates from a multiply transmitted, reflected and refracted signal ?

3.1 The magnitude of the reflected signal

Taking the air-glass interface as an example, at normal incidence there is approximately 96% transmission and 4% reflection at each boundary. Although the low 4% reflectance makes demands of the sensitivity of the TCSPC technique this is well within the dynamic range. The advantage is that as 96% of the light is transmitted the return from subsequent surfaces at normal incidence is only slightly diminished, for example the return of the eighth surface should only have fallen to about half of that from the first surface (allowing for go and return). However, common transparent materials like glass are often specularly reflective. This is a more severe problem since the return can typically fall off to 0.1% of the maximum at angles which are only 5 degrees from normal incidence. However, in the TCSPC system the dark count return is approximately 5×10^{-8} photons in a pulse width, so that the intensity of photon return can fall by at least four orders of magnitude without appreciably altering the statistical distribution of the true photon returns from the target. This assumes well separated surfaces. If the peaks are too close together then a small return can be "lost" in the tail of a more reflective surface.

3.2 Computing the depth coordinates

Next, we turn to the problem of depth determination. In general the laser pulse will be transmitted and reflected at a series of media boundaries; each photon scattered or reflected back along the transmission path may be registered in the photon count histogram. For simplicity and clarity of illustration the general case is described in two dimensions in figure 4, but the extension to three dimensions is straightforward. The laser pulse is transmitted from an optical origin $(x = 0, z = 0)$ at an angle of θ_0 to the z-axis. The laser impinges on a succession of m boundaries, b_i, at points $P_i(x_i, z_i)$ so that the angle of each boundary is θ_i measured clockwise from the x-axis and the refractive index of the next medium is n_i. The time of the measured return on the photon histogram from boundary b_i is t_i. The length of the path in the medium i is l_i. Allowing for the go-return path of the returned photons,

$$l_0 = \frac{c}{2n_0}t_0 \quad , \quad l_i = \frac{c}{2n_i}\left(t_i - \sum_{j=0}^{i-1} t_j\right) \tag{1}$$

where $c = 2.998 \times 10^8 m.s^{-1}$ is the speed of light in a vacuum. Applying Snell's law and defining the angle of refraction at b_i as θ_{ir} we can compute the coordinates of P_i, assuming that P_j are known for $j = 0$ to $i - 1$.

$$x_i = l_0 sin\theta_0 + \sum_{j=1}^{i} l_j sin(\theta_j + \theta_{jr}) \qquad z_i = l_0 cos\theta_0 + \sum_{j=1}^{i} l_j cos(\theta_j + \theta_{jr}) \tag{2}$$

The coordinates of the first surface can thus be determined without knowledge of the angle of incidence on the surface. However, each successive pair of coordinates is dependent on knowledge of the refractive index of the medium and the angle of incidence on the previous surface. Therefore it is necessary to define an iterative loop for computation of successive coordinates.

For each scan direction defined by θ_0
  Compute coordinates of P_0 (x_0, z_0)
  For each point on transmission path, P_i $(i = 1 \ to \ m)$
    Fit local surface to set of points surrounding P_{i-1}
    Hence, compute θ_{i-1}, x_i and z_i

4 Experimental results

In figure 3(b) we showed one example of a multiple return histogram from the floppy disk box illustrated in figure 2(a). In a separate experiment we scanned the sensor across the perspex block illustrated in figure 2(b). Unlike the floppy disk box the light travels from the air-perspex boundary through the perspex and emerges from the perspex-air boundary at the other side. In fact, the block was lying on its side when the profile was taken to avoid the opaque logo and backdrop. The speed of the light in the perspex block is reduced by the refractive index of the perspex block, which was measured to be ≈ 1.48.

Figure 5(a) shows one example of the photon return data from a single scan direction. The corresponding autocorrelation function is shown in figure 5(b). From this, the peak positions can be determined as 1504 and 1191 channels in front of the reference surface. A profile across the block is illustrated in figure 8(a). A panning head was used for the scan so that the vertical axis defines the channel position and the horizontal axis the angle of scan. Since the resolution of the MCA is 2.44ps/channel, this corresponds to to a time separation of $\approx 764ps$, or an optical path length, $n_i l_i \approx 228mm$. Allowing for the go-and-return path, this defines a path through the block of $\approx 7.7cm$. In fact, the thickness of the block is $7.6cm$ and this would not be altered much by the slight off-normal incidence of the scanning geometry. Within the limits of the experiment, this agreement is well within tolerance. Nevertheless, we acknowledge that a more careful experiment is required in which we use a material of exactly known refractive index and exact geometry, i.e. a carefully manufactured test piece.

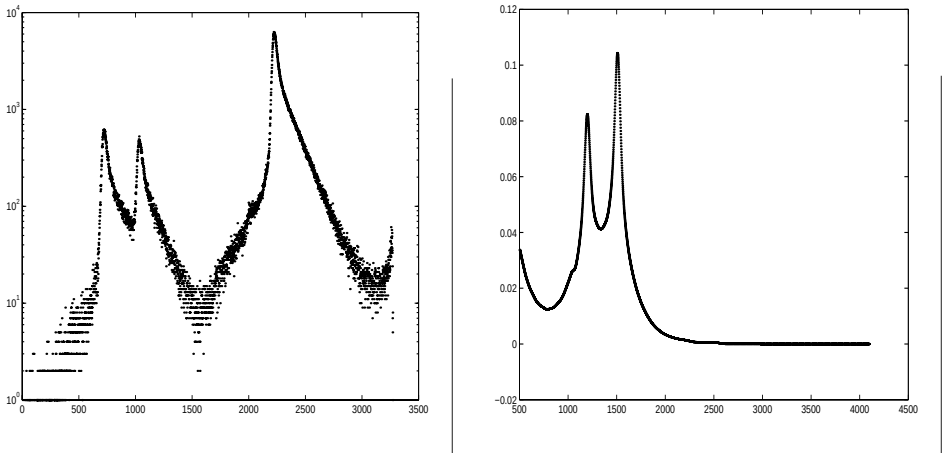

(a) Photon return histogram (b) Autocorrelation function

Figure 5: Measurements from front and rear surfaces of paperweight

We acquired complete 3D images of a number of glass and transparent plastic objects of varying size and shape. Figure 6(a) shows one example; this is a small symmetric Lego component with several planar faces at an angle to the incident beam and a single normal face with four studs used for attachment to other lego pieces. Figure 6(b) shows the depth data obtained from the test piece. The data is extremely irregular in comparison with data obtained from solid surfaces [6]. This can be better seen in a sample profile shown in figure 8(b); there are variations from the planar surface of 2mm. approximately with occasional outlying points which are as much as 1cm. from the true surface. This contrasts with the data from the opaque part of attaching block (on the right of the graph) which has much less variation. The profile was taken through two of the studs which can just be discriminated on the top surface. As intimated earlier, the variation in the data is a consequence of the variation in the return from the transparent object. Figures 7(a) and (b) show the data from a near-normal and angled part of the component respectively. In the latter case the photon return peaks at only 5 photons and does not provide as accurate a measure as we would like with current histogram interpretation techniques.

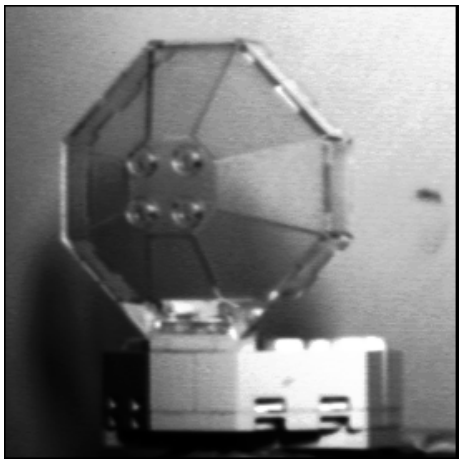

(a) Intensity image of Lego piece

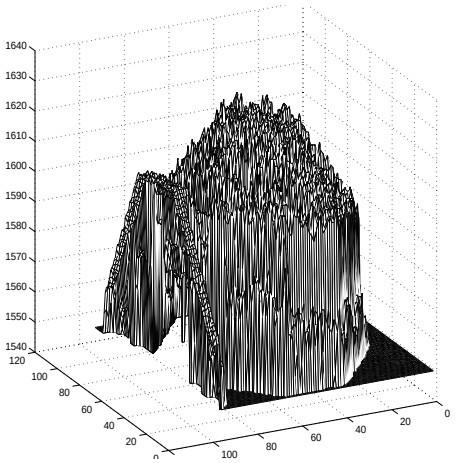

(b) Depth image of Lego piece

Figure 6: 3D scanning of front surface of transparent Lego object

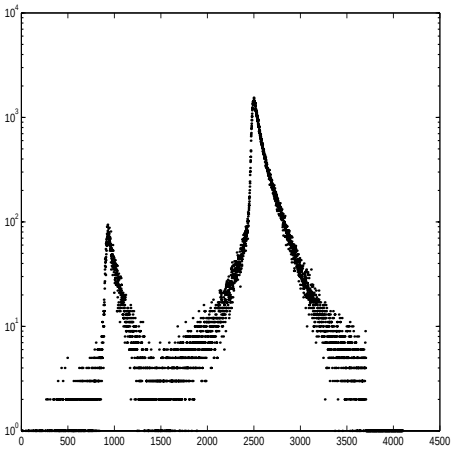

(a) 'Good' histogram

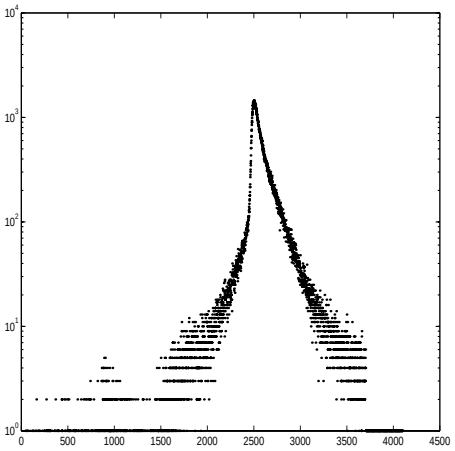

(b) 'Bad' histogram

Figure 7: 3D scanning of front surface of transparent Lego object

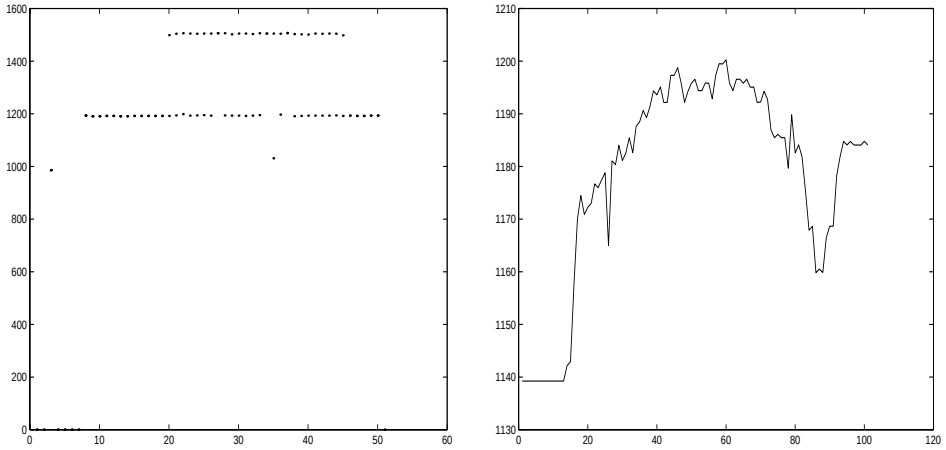

(a) Pattern Recognition paperweight (b) Lego component

Figure 8: Sample 3D profiles across scanned objects

5 Conclusions

We have made some initial progress towards measuring 3D data from transparent surfaces. In principle, it is possible to measure data from several surfaces simultaneously, but for some applications, it may only be necessary to measure data from the front surface. As an aside, we note that the technique could provide an alternative measurement of refractive index from a material of known dimensions.

The effectiveness of the procedure relies on the sensitivity of the time-correlated single photon counting technique. There are outstanding problems due to the specularity of many surfaces and the characteristic tail of the single photon avalanche diode. If a specular surface is at an oblique angle to the source ray then the photon peak may be very small. If two surfaces in the path of the incident ray are very close together the second return may be difficult to detect in the tail of the first.

Further work is necessary to see if the perceived limitations can be overcome. First one can consider the optomechanical design of the sensor. These measurements have been obtained with a sensor optimised to scan large opaque objects at a distance of 25 metres. There is obvious potential to acquire data with a smaller sensor, one in which the angle of the laser to the surface can be more closely controlled. Second one can consider the processing of the received data; the fit of the operating model has been shown to very accurate for histograms with significant numbers of returned photons [6]; in separate experiments on long range imaging [7] we have been considering how to better interpret the types of data shown in figure 7(b) but this work is ongoing.

References

[1] P.J. Besl. Active, optical range imaging sensors. *Machine Vision and Applications*, 1(2):127–152, 1988.

[2] T. Clarke. Simple scanners reveal shape, size and texture. *Optics and Lasers Europe*, May:29–32, 1998.

[3] M. Petrov, A. Talapov, T. Robertson, A. Lebedev, A. Zhilyaev, and L. Polonsky. Optical 3d digitizers: bringing life to the virtual world. In *IEEE Computer Graphics and Applications*, pages 28–37, 1998.

[4] J.S. Massa, G.S. Buller, A.C. Walker, S. Cova, M. Umasuthan, and A.M. Wallace. A time-of-flight optical ranging system using time-correlated single photon counting. *Applied Optics*, 37(31):7298–7304, 1998.

[5] D.V. O'Connor and D. Phillips. *Time-correlated single photon counting*. Academic Press, 1984.

[6] M. Umasuthan, A.M. Wallace, J. Massa, G.S. Buller, and A.C. Walker. Processing time-correlated single photon data to acquire range images. *IEE Proceedings: Vision, Image and Signal Processing*, 145(4):237–243, 1998.

[7] S. Pellegrini, G.S. Buller, A.M. Wallace, and S. Cova. laser based distance measurement using picosecond resolution time correlated single phton counting. *Measurement Sience and Technology*, 11, 2000.